RF Vision: RFID Receive Signal Strength Indicator (RSSI) Images for Sensor Fusion and Mobile Manipulation

Travis Deyle[1], Hai Nguyen[1], Matt Reynolds[2], and Charles C. Kemp[1]

[1]Healthcare Robotics Lab, Georgia Institute of Technology, USA
[2]Department of Electrical and Computer Engineering, Duke University, USA

Abstract—In this work we present a set of integrated methods that enable an RFID-enabled mobile manipulator to approach and grasp an object to which a self-adhesive passive (battery-free) UHF RFID tag has been affixed.

Our primary contribution is a new mode of perception that produces images of the spatial distribution of received signal strength indication (RSSI) for each of the tagged objects in an environment. The intensity of each pixel in the 'RSSI image' is the measured RF signal strength for a particular tag in the corresponding direction. We construct these RSSI images by panning and tilting an RFID reader antenna while measuring the RSSI value at each bearing. Additionally, we present a framework for estimating a tagged object's 3D location using fused ID-specific features derived from an RSSI image, a camera image, and a laser range finder scan.

We evaluate these methods using a robot with actuated, long-range RFID antennas and finger-mounted short-range antennas. The robot first scans its environment to discover which tagged objects are within range, creates a user interface, orients toward the user-selected object using RF signal strength, estimates the 3D location of the object using an RSSI image with sensor fusion, approaches and grasps the object, and uses its finger-mounted antennas to confirm that the desired object has been grasped.

In our tests, the sensor fusion system with an RSSI image correctly located the requested object in 17 out of 18 trials (94.4%), an 11.1% improvement over the system's performance when not using an RSSI image. The robot correctly oriented to the requested object in 8 out of 9 trials (88.9%), and in 3 out of 3 trials the entire system successfully grasped the object selected by the user.

I. INTRODUCTION

Radio frequency identification (RFID) is an umbrella term for a variety of transponder systems, including active (battery-powered) and passive (battery-free) tags of widely varying complexity and capabilities. In this work we concentrate on simple, low-cost passive UHF RFID tags, often called "smart labels," based on the widely adopted EPC Global Generation 2 communication protocol [1]. Currently available passive UHF RFID tags are battery-free, with a read range exceeding 5 meters and data storage capacities ranging from 128 bits to over 1K-bit. They currently cost less than $0.10 USD in volume. To date, RFID tags have typically been used in a purely binary fashion, returning tag IDs for each tag in range, or indicating that no tag was found. Prior work has shown how this binary tag sensing modality can be used to improve robot localization, mapping, navigation, and unique object detection.
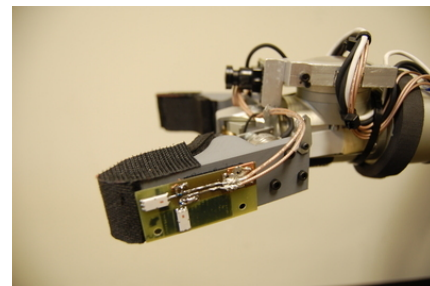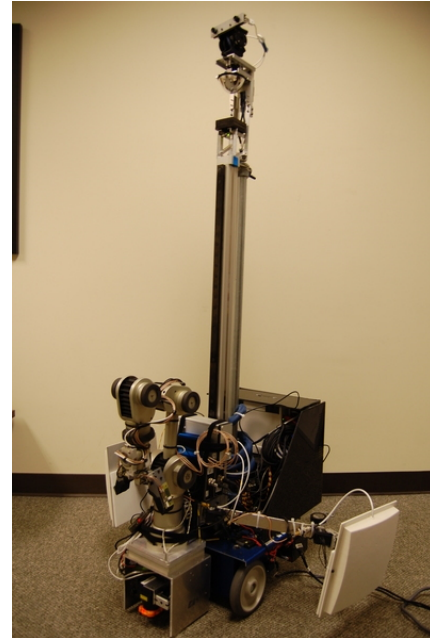

Fig. 1. The mobile manipulator, "EL-E" with two articulated, long range RFID antennas (top) and short-range near-field RFID antennas on the end effector (bottom).

Recent work has shown that there is valuable information present in the tag's RF signal itself, beyond the tag ID [2]. In our prior work, we have used estimates of received signal strength from passive RFID tags to inform robotic behaviors, both in the context of servoing an RFID-enabled robot toward a tagged object [3] and estimating a tag's position relative to the robot via particle filtering [4]. Here we present a new method for RFID-based sensing that uses the receive signal strength indication (RSSI) to form an RSSI image that can
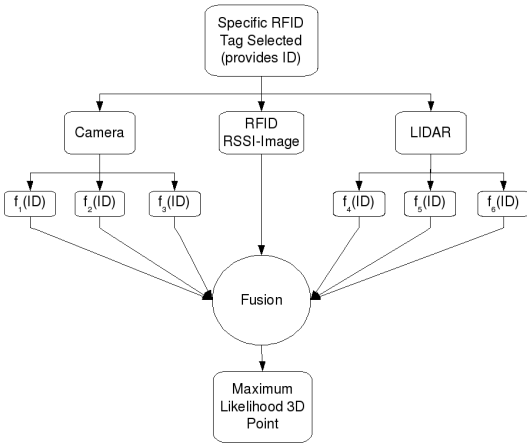
Fig. 2. Method for producing a maximum-likelihood 3D point estimate for the location of an RFID-tagged object

be fused with 2D images from a co-located camera and 3D point clouds from a co-located scanning laser range finder. We also show that the unique ID of a tag can be associated with perceptual characteristics of the object to which it is affixed, which in turn can facilitate object detection with this fused image. By combining the camera image, laser range finder scan, RSSI image, and object-specific data associated with this unique tag ID, our method is able to efficiently produce an estimate of the 3D location of a selected tagged object.

We have tested this approach in an object fetching application with EL-E, the autonomous mobile manipulator shown in Figure 1. In our tests, the robot first scans its environment to enumerate the tagged objects are in the environment. Based on the tag responses from the enumerated tagged objects, the robot then constructs a user interface from which the user can select an object to be fetched.

After selection, the robot servos its orientation such that the tagged object of interest is visible by both its camera and laser scanner. The servoing process maximizes the RSSI obtained from two long-range, actuated antennas reading the selected tag. The robot then constructs an RSSI image by panning and tilting one of these antennas and recording the RSSI signal for each bearing in terms of azimuth and elevation. The robot also captures an optical image with a calibrated color camera and a range scan using a tilting laser range finder. Each sensor's output is geometrically transformed to produce an output as a function of bearing in the robot's reference frame, so it is straightforward to fuse these three data sets into a single data set indexed by a single {azimuth, elevation} bearing pair. Additional features associated with each tagged object that have been associated with the tag's unique ID are read from a database and used to aid in finding the object in the fused image. This process results in a 3D estimate of the object's location, which the robot uses to approach and grasp the object using a system we have previously described [5], [6].

II. RELATED WORK

A wide variety of research has been conducted on the application of RFID technology to robotics. This includes RFID-enhanced interaction between robots and tagged people and objects, such as that described in [7], where tags facilitate person/object identification. There is also a great deal of prior work in RFID augmented indoor navigation [8], where tags are used as either a waypoint navigation and landmarking system [9], or more commonly as a component of a robot's localization and mapping system. Several recent works employ long-range passive UHF (902-928MHz) RFID, in addition to laser rangefinders and odometry, as sensor inputs to a probabilistic SLAM algorithm, for example [10]. In these prior results, the RFID system only reports the tag IDs of visible RFID tags, or indicates that no tag is found. In contrast, our work explicitly takes advantage of RF signal information.

An alternative RFID-enhanced navigation approach uses short-range ($\approx$1m) magnetically coupled passive RFID tags [11] to detect when robots pass above tagged waypoints. Again, however, a binary indication of tag presence or absence is all that is reported by the RFID system. Recent work in *active* (battery-powered) tagging [12] demonstrates navigation to a relatively expensive, battery powered target tag in a cluttered environment. In the latter work, a mechanically rotating reader antenna with a deep null in its radiation pattern is used to find bearings from the reader to the active tag. Other complex or expensive tag-centric antenna design techniques have also been explored to find range and bearing [13].

Numerous RFID tag localization approaches have been considered, including binary (read / no-read) histogram techniques [10] and RSSI techniques employing both histograms and sensor models, [2] and [4] respectively. While localization methods that estimate range and bearing posteriors may yield volumetric regions of interest, these methods tend to marginalize over the entire robot trajectory. We believe a compelling, potentially complementary, approach is to create 2D "images" of RF signal properties at a fixed robot location to provide valuable insights into the otherwise invisible RF world. To this end, we introduce RSSI images, shown in Figure 3, which capture the RSSI signal characteristics as a function of bearing (azimuth and elevation) in a manner analogous to an optical camera's visible light images.

In the fields of computer vision and augmented reality, there are many examples of systems that employ identifying fiducials, such as optical tags, coupled with a perceptual database. For example, QR codes have been used for both identification and 6DOF estimation for a manipulation task [14], while RFID tags have also been used in a database approach to identify perception and action primitives in a scene [15].

This work is differentiated in several ways: First, we believe this work to represent the first use of RSSI images as a distinct sensing modality. Further, we describe a probabilistic framework for sensor fusion, employing object-
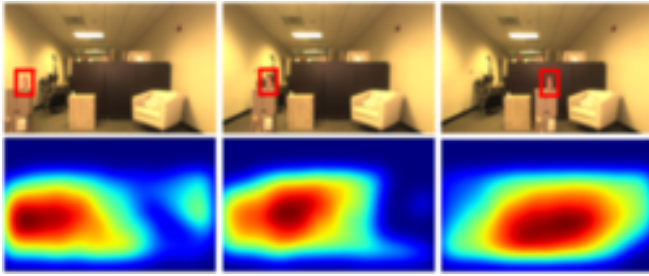
Fig. 3. Three camera images (top row) and corresponding blurred RSSI images (bottom row) of a tagged red bottle (marked with red box) as the bottle is moved from left to right across the scene. The strongest RSSI is depicted in red and corresponds with the location of the bottle in the images.
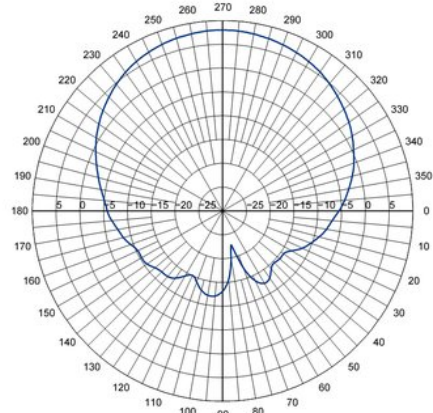

Fig. 4. A 2D slice of Cushcraft S9028PC antenna radiation pattern in polar format, with pan angle varying at a fixed tilt angle of $0°$. Peak antenna gain is ≈ 6.5dBi with a half-power beamwidth of $\approx 60°$.

centric features extracted from a database as indexed by the unique tag ID. Additionally, we demonstrate a user interface that allows users to select tagged objects from those present in the environment. Finally, we employ this framework to create a system capable of performing mobile manipulation of tagged objects.

III. RSSI IMAGES

Recent advances in RFID reader technology have made RF signal properties such as the Receive Signal Strength Indication (RSSI) available as metadata for each tag read by the reader. In its most basic form, RSSI is a scalar measurement of the tag's RF signal power as received at the reader. For example, we employ a ThingMagic Mercury 5e RFID reader which returns an RSSI value that is linearly related to received power in dBm. The raw reported RSSI value ranges from 70 to 100 units, though it saturates with very strong tag responses at a value of ≈ 105. Many system implementation and environmental factors affect the absolute value of the RSSI reported for a particular tag. We are primarily interested in RSSI variation with distance and bearing to each tag, but system implementation parameters such as transmit power, reader antenna characteristics, tag antenna characteristics also influence the absolute value of RSSI. In our work these system parameters are fixed, and do not vary with tag range and bearing. The RF properties of the robot's environment including occlusion, multipath, and interference are difficult to model and can also be significant, but we have found that they need not be modeled for nearby tags where line-of-sight propagation is dominant.

To construct an RSSI image, one of the robot's two long range, far-field RFID antennas is positioned in front of the robot, placing it approximately coincident with the tilting laser rangefinder and camera. The antenna is panned and tilted through azimuth and elevation angles while recording RSSI readings associated with a desired tag ID. A single slice of the radiation pattern for the antenna we employ, the Cushcraft S9028PC circularly polarized patch antenna, is illustrated in Figure 4. This antenna has horizontal and vertical half-power beamwidths of $\approx 60°$. This antenna beamwidth is the limiting factor in the precision of this sensor; advances in digitally scanned array antennas could

produce higher resolution images much faster than the pan-tilt mechanical scanning we are currently using. The resulting RSSI values are then mapped into a single image, roughly corresponding to a camera image. Next, the raw image is smoothed using a Gaussian filter with a standard deviation of 45 pixels, corresponding to $\approx 7°$ of pan or tilt. Lastly, the intensity values of the RSSI image are scaled to occupy the range [0.0, 1.0].

IV. SENSOR FUSION

The goal of our approach to sensor fusion is to combine the RSSI image for a particular tagged object ID with object-specific features extracted from other sensing modalities. We provide a probabilistic framework for fusing these sensing modalities and associated features to produce a single maximum likelihood 3D location that is used by the mobile manipulation system to retrieve the tagged object.

A. Registering the Sensors

In this work, we consider the output of three approximately coincident sensors with overlapping fields of view: the RSSI image, a low resolution (640x480) camera image from a rectified camera, and a 3D point cloud from a tilting laser rangefinder. In order to fuse the output of these three sensors, we first geometrically register them with one another. We accomplish this by transforming both the RSSI image and the 3D point cloud into the camera image.

For the 3D point cloud, we estimated the 6DOF transformation from the laser rangefinder to the camera by hand measurements, and then refined this estimate using visualization software that displays the transformed 3D point cloud on the corresponding camera image. Transforming the 3D point cloud results in a range image, $I_{range}(x, y)$, that is registered with the camera image, $I_{cam}(x, y)$.

For the RSSI image, we first convolve the raw RSSI image with a Gaussian, $G(\phi, \theta) * RSSI_{raw}(\phi, \theta)$, and then scale the resulting values to occupy the range [0.0, 1.0]. We then transform the resulting smoothed RSSI image into the

camera image with a simple linear interpolation based on hand measured correspondences between the RFID antenna's azimuth and elevation, (ϕ, θ), and the camera's pixels, (x, y). This results in the registered RSSI image, $I_{rssi}(x, y)$, as shown in Figure 3. Given the low spatial resolution of our current RSSI images and the near coincident location of the camera and antenna, this transformation is effective. However, we expect that more accurate registration would improve system performance.

B. Inferring a Tag's 2D Image Location

The fused image I consists of a set of n feature images $I_0...I_n$, where each feature image I_i represents the spatially varying value of feature F_i. We model each of these features as being generated with some probability $p_{f_i|tag}(F_i, \text{True})$, if a tag is at the bearing associated with the location. If a tag is not at the bearing associated with the location, we model the probability of a given feature value as $p_{f_i|tag}(F_i, \text{False})$. We further model these feature values as being conditionally independent given the presence or absence of the tag at the bearing associated with the location, and as independent from one another. Given these assumptions, we can find the probability that a tag is at a given location using Bayes' rule:

$$p_{tag|f_0...f_n}(V, F_0...F_n) = \frac{p_{f_0...f_n|tag}(F_0...F_n, V)p_{tag}(V)}{p_{f_0...f_n}(F_0...F_n)} \quad (1)$$

$$= \frac{\left(\prod_{i=1}^{n} p_{f_i|tag}(F_i, V)\right) p_{tag}(V)}{\prod_{i=1}^{n} p_{f_i}(F_i)} \quad (2)$$

$$= p_{tag}(V) \prod_{i=1}^{n} \frac{p_{f_i|tag}(F_i, V)}{p_{f_i}(F_i)} \quad (3)$$

We assume a uniform prior on the position of each tag, $p_{tag}(V)$. Assuming independence of the feature vectors for each x, y location of the fused image I, $p_{image}(I) = \prod p_{f_0...f_n|tag}(I(x, y), V(x, y))$. And,

$$p_{f_i}(I_i(x, y)) = p_{f_i|tag}(I_i(x, y), \text{True}) + \quad (4)$$
$$p_{f_i|tag}(I_i(x, y), \text{False}).$$

The maximum likelihood (ML) estimate of the location of the tag is then

$$argmax_{x,y} \left\{ \prod_{i=1}^{n} \frac{p_{f_i|tag}(I_i(x, y), \text{True})}{p_{f_i}(I_i(x, y))} \right\}. \quad (5)$$

The result of this $argmax$ operation selects a pixel, (x_{ml}, y_{ml}), in the fused image. In the subsequent section, we will show how this pixel may be mapped into the 3D point cloud produced by the tilting laser range finder to produce a single maximum-likelihood 3D location for the tagged object. This interaction is illustrated in Figure 2.

C. Inferring a Tag's 3D Location

In order to effectively apply this method of probabilistic inference, we select discriminative feature(s) from each sensing modality. The selection of discriminating features could employ feature sets, models, and / or training data available from a database indexed by the tag's ID. In this work, we consider three features indexed by tag ID. First, the feature from the RSSI image consists of the RSSI value from $I_{rssi}(x, y)$. The associated probabilities, $p_{rssi|tag}(RSSI, \text{True})$ and $p_{rssi|tag}(RSSI, \text{False})$, were obtained as a histogram from 60 hand-labeled ground-truth observations as shown in Figure 5. From the camera image, we employed color histograms as the visual feature. We selected color histograms for their simplicity. Other visual features could be integrated into this framework and may be more discriminative. For the color histogram, the object probability, $p_{color|tag}(I_{cam}(x, y), \text{True})$, is obtained from an image of the tagged object stored in the tag-indexed database. Meanwhile, the non-object background probability, $p_{color|tag}(I_{cam}(x, y), \text{False})$, is generated from a color histogram accumulated over the set of images of the environment collected during navigation.

For the laser, there are many candidate features, from spin images [16] to 3D segmentations as applied in our previous work [17]. In this work we have treated the laser as a special case, where point 3D ($p3d$) features are used to produce a binary mask on the image:

$$\frac{p_{p3d|tag}(P3D, V)}{p_{p3d}(P3D)} = \begin{cases} 1.0 & P3D \in \text{laser scan} \\ 0.0 & \neg P3D \in \text{laser scan} \end{cases}$$

This ensures that any pixel selected by $argmax_{x,y}$ produces a direct mapping to a valid 3D location based on laser range scans. After all three sensor images are fused, the maximum likelihood pixel is selected, and the corresponding 3D location from the laser is chosen. A montage showing this method is shown in Figure 6.

V. Mobile Manipulation System

The fused sensor image is incorporated as follows into the mobile manipulation system. The robot first uses the RFID antennas to scan the environment for tagged objects in the environment. The object names associated database images corresponding to each tag ID are presented to a remote user via the graphical user interface shown in Figure 7. The user can select an object from an array of database photos, indexed by the observed tag ID of each tagged object. After the user selects a tagged object, the robot estimates a bearing to the tag of interest. The robot rotates to that bearing, placing the object within the other sensors' field of view. The robot proceeds by performing sensor fusion as previously described, which results in a 3D estimate of the object's location. The robot then uses the 3D estimate of the object's location to approach and grasp the object using an overhead grasp with methods we have previously described [5], [6], [17]. Finally, after the grasp attempt is completed, the RFID antennas in the robot's end effector (see Figure 1) are used to determine success or failure by
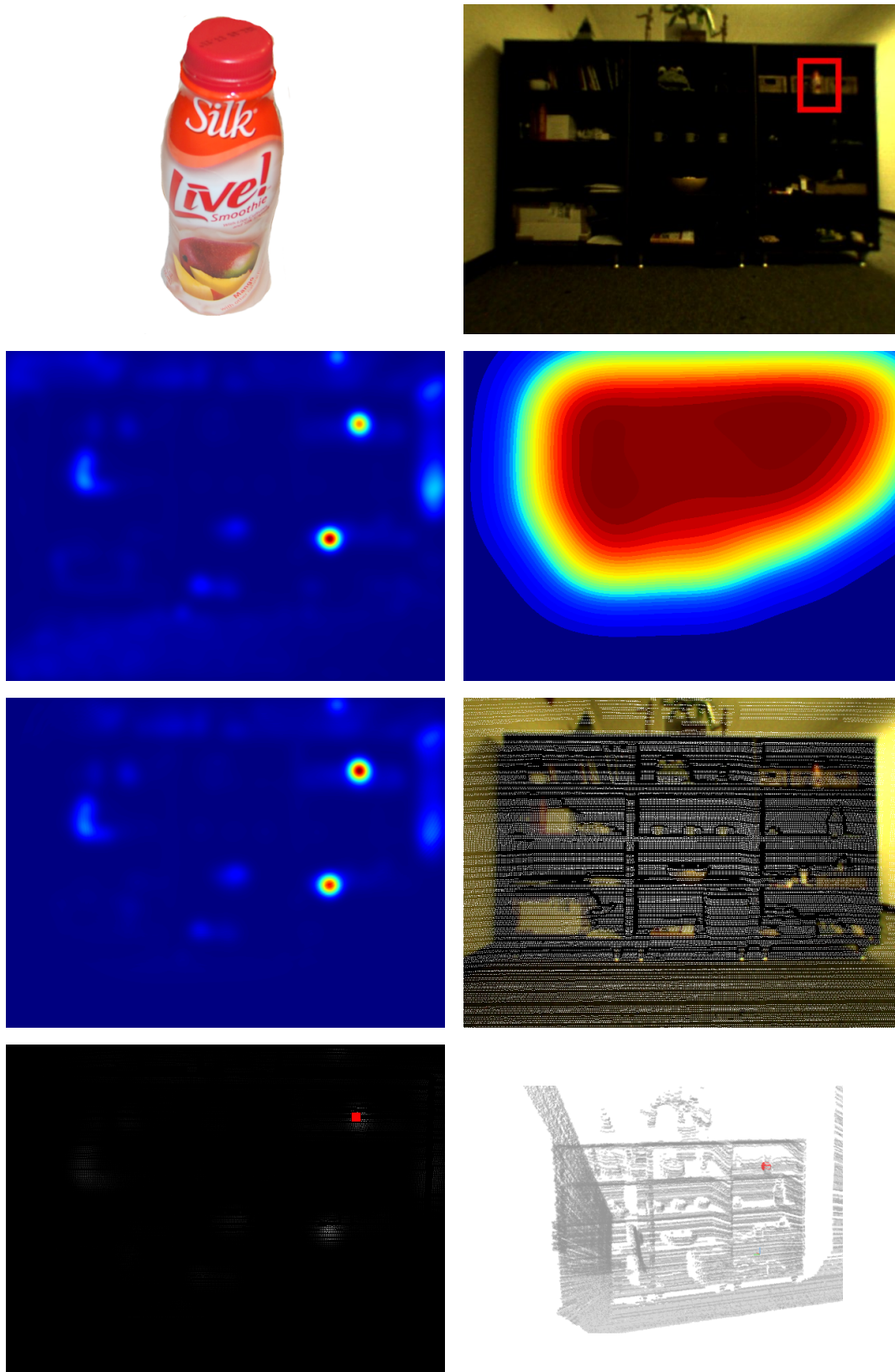
Fig. 6. Intermediate steps to selecting a beverage bottle. From top to bottom, left to right: The desired object, the raw camera image with the bottle highlighted, the camera probability image, the RSSI probability image, the intermediate fusion result, the laser rangefinder "mask" probability (shown as white points in the image), the selected pixel in red, and the projection of this pixel back into the 3D laser rangefinder data. *Note:* In this example, the fused result is correct, while the color histogram alone is ambiguous and yields an incorrect result.
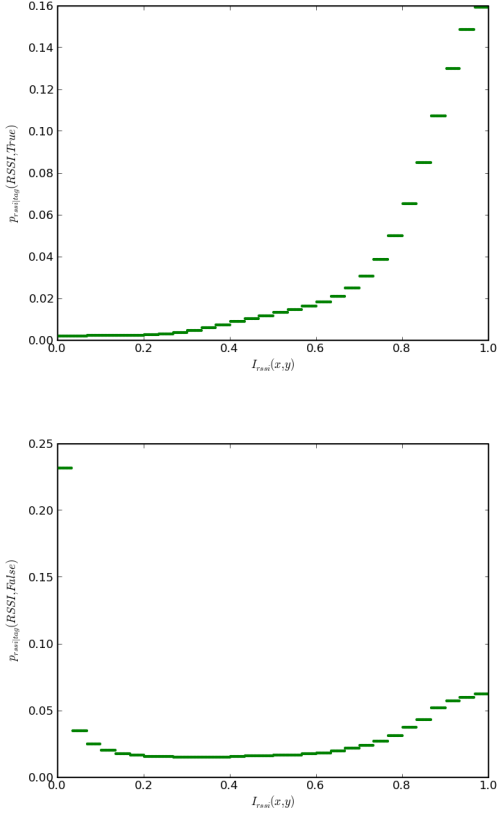
Fig. 5. RSSI feature probability distributions determined from 60 hand-labeled training examples. $p_{rssi|tag}(RSSI, \text{True})$ is on the top; $p_{rssi|tag}(RSSI, \text{False})$ is on the bottom.

confirming the tag ID of the object being grasped. In our experimental work thus far, we classify experimental trials as successes or failures depending on whether the correct object is successfully grasped.

A. Bearing Estimation

In order to successfully fuse images from multiple sensors, the robot must servo its pose so that the field of view of all sensors includes the desired object. In previous work we rotated the robot toward the tagged object by maximizing selected-tag RSSI from an antenna mounted at a fixed pose on the robot [3]. In the present work the pan/tilt antennas mounted on the robot permit keeping the robot in a fixed position while scanning only the RFID antennas. The RSSI values from the two pan/tilt antennas are combined to form a dataset of RSSI versus robot bearing. We obtain the bearing from the robot to the tag by fitting to a second-order exponential parameterized by $[\alpha, \mu, \sigma, \beta]^T$ using least squares:

$$argmax_x \left\{ \alpha \cdot e^{-(x-\mu)^2/\sigma} + \beta \right\} \tag{6}$$

This operation is shown graphically in Figure 8. The bearing process is repeated twice to account for the uncertainty behind the robot where the articulated antennas cannot sense tags due to mechanical interference with the robot's body.
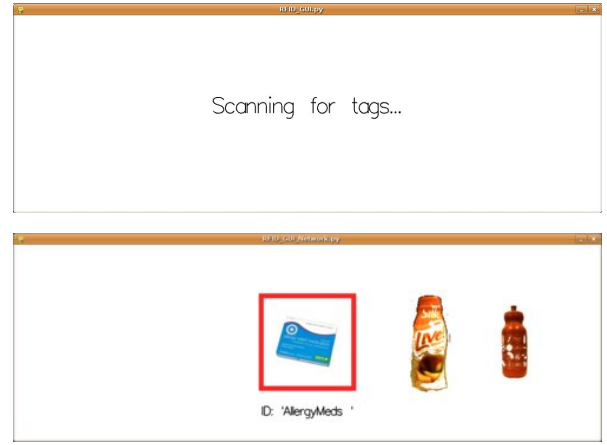

Fig. 7. Dynamically generated user interface presenting a menu of tagged objects available to be grasped by the robot.
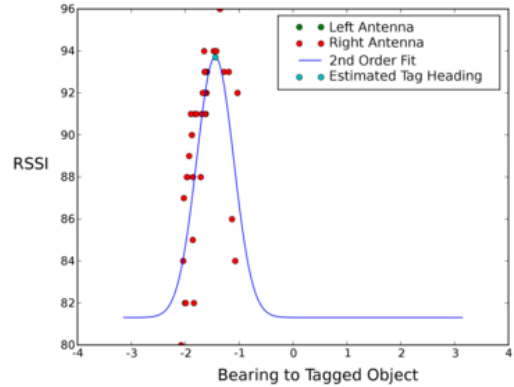

Fig. 8. RSSI readings from the two antennas (in this instance, the left antenna had no reads) fitted with a 2nd order exponential function. The $argmax\{\theta\}$ from this fit is the estimated bearing to the tagged object.

VI. RESULTS

A. Evaluating 3D Location Estimation

We performed a number of tests of the sensor fusion system's accuracy when estimating tagged object locations in 3D. For our test scenario, we chose three objects with distinct color histograms: a red water bottle, a blue medication box, and an orange disposable beverage bottle, shown in the top of Figure 9. We chose two cluttered but unobstructed scenes and three locations (shown in Figure 9) within each scene where each of the three objects was tested, resulting in a total of 18 3D location estimation trials. The algorithm from Figure 6 was executed for each trial and was deemed successful if the 3D point derived from the fused image belonged to the desired object. The 3D location estimation was successful in 17 of the 18 trials (94.4%), with the only failure occurring for the orange disposable drink bottle due to a proximal orange distractor in the color histogram image. It is worth noting that the success rate *without* the RSSI image on the same dataset was 15 of 18 (83.3%); thus, incorporation of the RSSI image resulted in an 11.1% improvement in the system's performance.

Fig. 9. Three test objects: red water bottle, blue medication box, and orange disposable bottle (top). The two scenes and their three associated object placement locations are indicated. The sole failure occurred when the orange disposable bottle was placed in the upper-right placement location in the bottom scene.

Fig. 10. Three different bearing estimation scenarios, with object locations highlighted. Bearing estimation was attempted for all three objects, each in the three different locations (9 total attempts). In 8 of 9 instances, the robot correctly achieved a bearing that placed the tagged object in the fused sensor image.

B. Evaluating Bearing Estimation

We tested bearing estimation in 3 different positions, for the same three objects used in the fused image experiments. The bearing estimation cases, illustrated in Figure 10 where successful in 8 of 9 trials (88.9%), where success was defined by halting with the desired object within fused image's field of view.

C. Evaluating Mobile Manipulation

We performed three tests of the entire mobile manipulation system. In all three trials, the robot successfully grasped the correct object and verified the ID of the object post-grasp using the RFID antennas in the manipulator (see Figure 1).

VII. LIMITATIONS AND FUTURE WORK

The methods we propose have a variety of limitations which may be mitigated in future work. The performance of RFID tags can vary considerably depending on their orientation, the materials composing the object, and the RF properties of the environment (e.g., transmission, absorption,

reflection, multipath interactions, etc.). We expect that issues with orientation and some forms of environmental obstruction can be mitigated by affixing multiple tags to the same object, or by using recently-developed UHF RFID tags with improved omnidirectional performance. Recently developed UHF RFID tags have also been introduced for challenging object materials, including metal objects which would not work well with the tags we used in our experiments.

Faster methods to acquire scanned RFID data, including digitally scanned antenna arrays, would have a variety of advantages, including the ability to handle dynamic environments and make additional estimates from different perspectives. We expect that flash LIDAR "range cameras" and digitally scanned RFID antenna arrays could achieve performance at rates that are comparable to conventional video camera framerates. Being able to quickly make additional estimates from various perspectives would be advantageous for overcoming environmental RF issues and could be inte-
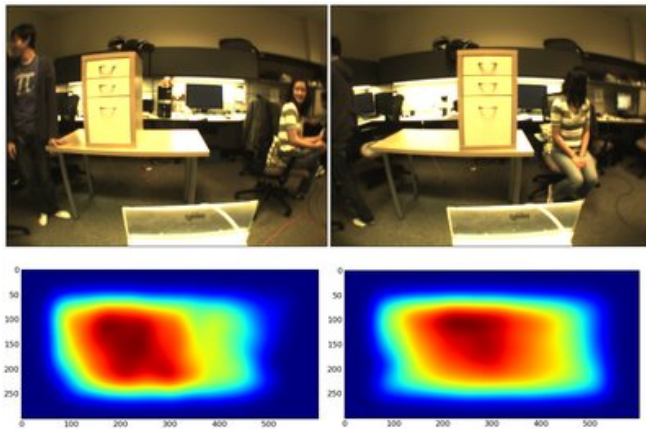
Fig. 11. Two camera images (top row) and corresponding Gaussian-filtered RSSI images (bottom row) of a tagged bottle inside the top drawer of a wooden cabinet being moved from left to right. The strongest RSSI signals are depicted in red and correspond with the location of the bottle in the images.

grated into 3D estimation techniques related to our previous work on particle filters [4].

The choice of discriminating features for each sensing modality is critical to the robustness of the system. In this work we used color histograms as a straightforward example, but an unfavorable environment could easily lead to confusion. For future work, we plan to incorporate additional descriptive features from the various sensing modalities. Further, as shown in Figure 11, the RSSI is informative even when the remaining sensors cannot perceive the desired object. We believe this represents an interesting avenue for further research.

VIII. CONCLUSIONS

We have presented an integrated set of methods that enable a mobile manipulator to grasp an object to which a self-adhesive UHF RFID tag has been affixed. Among other contributions, we have introduced the use of RSSI images to help detect and localize tagged objects, along with a framework for estimating a tagged object's 3D location using a fused sensory representation and sensory features associated with the unique identifier obtained from the object's RFID tag.

We evaluated our methods using a robot that first scans an area to discover which tagged objects are within range, creates a user interface, orients to the user-selected object using RF signal strength, estimates the 3D location of the object using an RSSI image with sensor fusion, approaches and grasps the object, and then uses its finger-mounted antennas to confirm that the desired object has been grasped.

This work demonstrates that RFID-based perception has the potential to become integral to all aspects of mobile manipulation including the discovery of what objects are available, the production of customized user interfaces, the navigation of the robot to objects, and the manipulation of objects.

REFERENCES

[1] EPC Global US, "Class 1 Generation 2 UHF RFID protocol for operation at 860MHz-960MHz, version 1.0.9," Available online, *http://www.epcglobalus.org/*.

[2] D. Joho, C. Plagemann, and W. Burgard, "Modeling RFID Signal Strength and Tag Detection for Localization and Mapping," in *IEEE international conference on robotics and automation*, 2009.

[3] T. Deyle, C. Anderson, C. C. Kemp, and M. S. Reynolds, "A foveated passive UHF RFID system for mobile manipulation," *Intelligent Robots and Systems, 2008. IROS 2008. IEEE/RSJ International Conference on*, pp. 3711–3716, 2008.

[4] T. Deyle, C. C. Kemp, and M. S. Reynolds, "Probabilistic UHF RFID tag pose estimation with multiple antennas and a multipath RF propagation model," *Intelligent Robots and Systems, 2008. IROS 2008. IEEE/RSJ International Conference on*, pp. 1379–1384, 2008.

[5] Y. S. Choi, C. D. Anderson, J. D. Glass, and C. C. Kemp, "Laser pointers and a touch screen: Intuitive interfaces to an autonomous mobile robot for the motor impaired," in *ACM SIGACCESS Conference on Computers and Accessibility*, 2008.

[6] H. Nguyen, C. D. Anderson, A. J. Trevor, A. Jain, Z. Xu, and C. C. Kemp, "El-e: An assistive robot that fetches objects from flat surfaces," in *Robotic Helpers, Int. Conf. on Human-Robot Interaction*, 2008.

[7] M. Shiomi, T. Kanda, H. Ishiguro, and N. Hagita, "Interactive humanoid robots for a science museum," in *Proceedings of ACM SIGCHI/SIGART Conference on Human-Robot Interaction*. New York, NY, USA: ACM, 2006, pp. 305–312.

[8] O. Kubitz, M. Berger, M. Perlick, and R. Dumoulin, "Application of radio frequency identification devices to support navigation of autonomous mobile robots," in *Proceedings of IEEE 47th Vehicular Technology Conference*, vol. 1, 4-7 May 1997, pp. 126–130.

[9] V. Kulyukin, C. Gharpure, J. Nicholson, and S. Pavithran, "RFID in robot-assisted indoor navigation for the visually impaired," in *Proceedings of IEEE/RSJ International Conference on Intelligent Robots and Systems*, vol. 2, 28 Sept.-2 Oct. 2004, pp. 1979–1984.

[10] D. Hahnel, W. Burgard, D. Fox, K. Fishkin, and M. Philipose, "Mapping and localization with RFID technology," in *Proceedings of IEEE International Conference on Robotics and Automation*, vol. 1, 26 April-1 May 2004, pp. 1015–1020.

[11] V. Ziparo, A. Kleiner, B. Nebel, and D. Nardi, "RFID-based exploration for large robot teams," in *Proceedings of IEEE International Conference on Robotics and Automation*, 10-14 April 2007, pp. 4606–4613.

[12] M. Kim, H. W. Kim, and N. Y. Chong, "Automated robot docking using direction sensing RFID," in *Proceedings of IEEE International Conference on Robotics and Automation*, 10-14 April 2007, pp. 4588–4593.

[13] Se–gon Roh, Y. H. Lee, and H. R. Choi, "Object recognition using 3D tag-based RFID system," in *Proceedings of IEEE/RSJ International Conference on Intelligent Robots and Systems*, Oct. 2006, pp. 5725–5730.

[14] R. Katsuki, J. Ota, Y. Tamura, T. Mizuta, T. Kito, T. Arai, T. Ueyama, and T. Nishiyama, "Handling of objects with marks by a robot," *Intelligent Robots and Systems, 2003. (IROS 2003). Proceedings. 2003 IEEE/RSJ International Conference on*, vol. 1, pp. 130–135 vol.1, Oct. 2003.

[15] N. Y. Chong, H. Hongu, K. Ohba, S. Hirai, and K. Tanie, "A distributed knowledge network for real world robot applications," *Intelligent Robots and Systems, 2004. (IROS 2004). Proceedings. 2004 IEEE/RSJ International Conference on*, vol. 1, pp. 187–192 vol.1, Sept.-2 Oct. 2004.

[16] A. Johnson and M. Hebert, "Using spin images for efficient object recognition in cluttered 3d scenes," *Pattern Analysis and Machine Intelligence, IEEE Transactions on*, vol. 21, no. 5, pp. 433–449, May 1999.

[17] A. Jain and C. C. Kemp, "Behavior-based door opening with equilibrium point control," in *RSS Workshop: Mobile Manipulation in Human Environments*, 2009.